Correspondence

Semi-Blind SIMO Flat-Fading Channel Estimation in Unknown Spatially Correlated Noise Using the EM Algorithm

Aleksandar Dogandžić, Wei Mo, and Zhengdao Wang

***Abstract*—We present a maximum likelihood (ML) method for semi-blind estimation of single-input multi-output (SIMO) flat-fading channels in spatially correlated noise having unknown covariance. An expectation–maximization (EM) algorithm is utilized to compute the ML estimates of the channel and spatial noise covariance. We derive the Cramér–Rao bound (CRB) matrix for the unknown parameters and present a symbol detector that utilizes the EM channel estimates. Numerical simulations demonstrate the performance of the proposed method.**

***Index Terms*—Array processing, Cramér–Rao bound, EM algorithm, semi-blind channel estimation, spatial interference suppression.**

I. Introduction

The expectation–maximization (EM) and related algorithms (see [1]–[3]) have been applied to carrier phase recovery [4], demodulation for unknown carrier phase [5], timing estimation [6], and channel estimation [7]–[9] in single-input single-output (SISO) communication systems and, more recently, to symbol detection [10]–[12] and channel estimation [13]–[15] in *smart-antenna* systems. In this paper (see also [17]), we treat the unknown symbols as the *unobserved* (or missing) data and propose an EM algorithm for semi-blind maximum likelihood (ML) estimation of *both* the channel and spatial noise covariance in a single-input multi-output (SIMO) smart antenna scenario. This is unlike previous work in [7]–[9] and [13]–[15], where EM algorithms were applied to channel estimation in white noise.

The signal and noise models are introduced in Section II. In Section III, we derive the EM algorithm for estimating the unknown channel and noise parameters, and in Section IV, we compute the Cramér–Rao bound (CRB) matrix for these parameters. The EM channel estimates are incorporated into the receiver design in Section V. We present numerical examples in Section VI and conclude the paper in Section VII.

II. Measurement Model

Consider a single-input multi-output (SIMO) flat-fading channel with equiprobable constant-modulus symbols. Denote by $\boldsymbol{y}(t)$ an $n_{\mathrm{R}} \times 1$ data vector (snapshot) received by an array of n_{R} antennas at time t and assume that we have collected N snapshots from a coherent interval containing the unknown symbols. Under a single-user slow flat-fading scenario, $\boldsymbol{y}(t)$ can be modeled as

$$\boldsymbol{y}(t) = \boldsymbol{h} \cdot u(t) + \boldsymbol{e}(t), \quad t = 1, 2, \ldots, N \tag{2.1}$$

where

- $\boldsymbol{h}$ unknown $n_{\mathrm{R}} \times 1$ channel response vector;
- $u(t)$ unknown symbol received by the array at time t;
- $\boldsymbol{e}(t)$ temporally white and circularly symmetric zero-mean complex Gaussian noise vector with unknown positive definite spatial covariance matrix Σ.

The channel $\boldsymbol{h}$ and noise covariance matrix Σ are assumed to be constant for $t \in \{1, 2, \ldots, N\}$. The spatially correlated noise model accounts for co-channel interference (CCI) and receiver noise.[1] We further assume that the symbols $u(t)$ belong to an M-ary constant-modulus constellation

$$\mathcal{U} = \{u_1, u_2, \ldots, u_M\} \tag{2.2a}$$

where

$$|u_m| = 1, \quad m = 1, 2, \ldots, M. \tag{2.2b}$$

(The constant-modulus assumption can be relaxed; see Appendix A.) We model $u(t), t = 1, 2, \ldots, N$ as independent, identically distributed (i.i.d.) random variables with probability mass function

$$p(u(t)) = \frac{1}{M}\, i(u(t)) \tag{2.3}$$

where

$$i(u) = \begin{cases} 1, & u \in \mathcal{U} \\ 0, & \text{otherwise.} \end{cases} \tag{2.4}$$

Our goal is to estimate the unknown channel and noise parameters $\boldsymbol{h}$ and Σ. To allow unique estimation of the channel $\boldsymbol{h}$ (e.g., to resolve the phase ambiguity), we further assume that N_{T} *known* (training) symbols

$$u_{\mathrm{T}}(\tau) \in \mathcal{U}, \quad \tau = 1, 2, \ldots, N_{\mathrm{T}} \tag{2.5}$$

are embedded in the transmission scheme and denote the corresponding snapshots received by the array as $\boldsymbol{y}_{\mathrm{T}}(\tau), \tau = 1, 2, \ldots, N_{\mathrm{T}}$. Then, the measurement model (2.1) holds for the training symbols as well, with $\boldsymbol{y}(t)$ and $u(t)$ replaced by $\boldsymbol{y}_{\mathrm{T}}(\tau)$ and $u_{\mathrm{T}}(\tau)$, respectively.

In the following, we present an EM algorithm for computing the ML estimates of $\boldsymbol{h}$ and Σ under the above measurement model.

III. ML Estimation

The EM algorithm is a general iterative method for computing ML estimates in the scenarios where ML estimation cannot be easily performed by directly maximizing the likelihood function of observed measurements. Each EM iteration consists of maximizing the expected complete-data log-likelihood function, where the expectation is computed with respect to the conditional distribution of the unobserved data given the observed measurements. A good choice of unobserved data allows easy maximization of the expected complete-data log-likelihood. The algorithm converges monotonically to a local or the global maximum of the observed-data likelihood function; see, e.g., [3, ch. 3]. Here, the unknown symbols $u(t), t = 1, 2, \ldots, N$ are modeled as the unobserved (or missing) data. Given $u(t)$, the corresponding *observed*

[1]This noise model has been used in numerous recent publications to account for unstructured interference; see, e.g., [18] and references therein.

Manuscript received May 29, 2003; revised August 9, 2003. The associate editor coordinating the review of this manuscript and approving it for publication was Prof. Zhi Ding.

The authors are with the Department of Electrical and Computer Engineering, Iowa State University, Ames, IA 50011 USA (e-mail: ald@iastate.edu; mowei@iastate.edu; zhengdao@iastate.edu).

Digital Object Identifier 10.1109/TSP.2004.827200

snapshot $\boldsymbol{y}(t)$ is distributed as a complex multivariate Gaussian vector with probability density function (pdf)

$$f(\boldsymbol{y}(t)|u(t),\boldsymbol{h},\Sigma) = \frac{1}{|\pi\Sigma|}\cdot\exp\left\{-[\boldsymbol{y}(t)-\boldsymbol{h}u(t)]^H\Sigma^{-1}[\boldsymbol{y}(t)-\boldsymbol{h}u(t)]\right\} \quad (3.1)$$

where "^{H}" denotes the Hermitian (conjugate) transpose. The above expression also holds for the training data, with $\boldsymbol{y}(t)$ and $u(t)$ replaced by $\boldsymbol{y}_{\mathrm{T}}(\tau)$ and $u_{\mathrm{T}}(\tau)$. The joint distribution and mass function of $\boldsymbol{y}(t)$, $u(t)$ (for $t=1,2,\ldots,N$) and $\boldsymbol{y}_{\mathrm{T}}(\tau)$ (for $\tau=1,2,\ldots,N_{\mathrm{T}}$) can be written as

$$\prod_{t=1}^{N} p(u(t))f(\boldsymbol{y}(t)|u(t),\boldsymbol{h},\Sigma)\cdot\prod_{\tau=1}^{N_{\mathrm{T}}} f(\boldsymbol{y}_{\mathrm{T}}(\tau)|u_{\mathrm{T}}(\tau),\boldsymbol{h},\Sigma) \quad (3.2)$$

which is also known as the *complete-data likelihood function* . The *observed-data likelihood function* to be maximized is then

$$\begin{aligned}&\Big[\sum_{u(1)\in\mathcal{U}}\sum_{u(2)\in\mathcal{U}}\cdots\sum_{u(N)\in\mathcal{U}}\prod_{t=1}^{N}p(u(t))\\&\quad\cdot f(\boldsymbol{y}(t)|u(t),\boldsymbol{h},\Sigma)\Big]\\&\quad\cdot\prod_{\tau=1}^{N_{\mathrm{T}}} f(\boldsymbol{y}_{\mathrm{T}}(\tau)|u_{\mathrm{T}}(\tau),\boldsymbol{h},\Sigma)\\&\quad=\prod_{t=1}^{N}\left[\sum_{m=1}^{M}\frac{1}{M}\cdot f(\boldsymbol{y}(t)|u_m,\boldsymbol{h},\Sigma)\right]\\&\qquad\cdot\prod_{\tau=1}^{N_{\mathrm{T}}} f(\boldsymbol{y}_{\mathrm{T}}(\tau)|u_{\mathrm{T}}(\tau),\boldsymbol{h},\Sigma).\end{aligned} \quad (3.3)$$

In Appendix A, we derive the EM algorithm for maximizing (3.3): Iterate between the following.

Step 1)

$$\boldsymbol{h}^{(k+1)} = \frac{1}{N+N_{\mathrm{T}}}\left\{\sum_{t=1}^{N}\left[\boldsymbol{y}(t)\sum_{m=1}^{M}u_m^*\cdot\rho_m^{(k)}(t)\right]+\sum_{\tau=1}^{N_{\mathrm{T}}}\boldsymbol{y}_{\mathrm{T}}(\tau)u_{\mathrm{T}}(\tau)^*\right\} \quad (3.4a)$$

where

$$\rho_m^{(k)}(t)=\frac{\exp\left\{-\left[\boldsymbol{y}(t)-\boldsymbol{h}^{(k)}u_m\right]^H(\Sigma^{(k)})^{-1}\left[\boldsymbol{y}(t)-\boldsymbol{h}^{(k)}u_m\right]\right\}}{\sum_{n=1}^{M}\exp\left\{-\left[\boldsymbol{y}(t)-\boldsymbol{h}^{(k)}u_n\right]^H(\Sigma^{(k)})^{-1}\left[\boldsymbol{y}(t)-\boldsymbol{h}^{(k)}u_n\right]\right\}}. \quad (3.4b)$$

Step 2)

$$\Sigma^{(k+1)} = R_{yy}-\boldsymbol{h}^{(k+1)}(\boldsymbol{h}^{(k+1)})^H. \quad (3.5)$$

Here

$$R_{yy}=\frac{1}{N+N_{\mathrm{T}}}\left[\sum_{t=1}^{N}\boldsymbol{y}(t)\boldsymbol{y}(t)^H+\sum_{\tau=1}^{N_{\mathrm{T}}}\boldsymbol{y}_{\mathrm{T}}(\tau)\boldsymbol{y}_{\mathrm{T}}(\tau)^H\right] \quad (3.6)$$

is the sample correlation matrix of the observed data, and "*" denotes complex conjugation. Note that the terms in the summation over t in (3.4a) can be computed in parallel. To ensure that the estimates of the spatial noise covariance matrix in (3.5) are positive definite with probability one, the following condition should be satisfied:

$$N+N_{\mathrm{T}}\geq n_{\mathrm{R}}+1 \quad (3.7)$$

(see also the discussion in Appendix A). Expression (3.4b) can be further simplified by canceling out terms in the numerator and denominator:

$$\rho_m^{(k)}(t)=\frac{\exp\left[2\mathrm{Re}\left\{\boldsymbol{y}(t)^H(\Sigma^{(k)})^{-1}\boldsymbol{h}^{(k)}u_m\right\}\right]}{\sum_{n=1}^{M}\exp\left[2\mathrm{Re}\left\{\boldsymbol{y}(t)^H(\Sigma^{(k)})^{-1}\boldsymbol{h}^{(k)}u_n\right\}\right]} \quad (3.8)$$

where we have used the constant-modulus property of the transmitted symbols. In the $(k+1)$st iteration, Step 2 requires computing $(\Sigma^{(k)})^{-1}$, which can be done using the matrix inversion lemma in, e.g., [20, Cor. 18.2.10]:

$$(\Sigma^{(k)})^{-1}=R_{yy}^{-1}+\frac{R_{yy}^{-1}\boldsymbol{h}^{(k)}(\boldsymbol{h}^{(k)})^HR_{yy}^{-1}}{1-(\boldsymbol{h}^{(k)})^HR_{yy}^{-1}\boldsymbol{h}^{(k)}} \quad (3.9a)$$

where R_{yy}^{-1} needs to be evaluated only once before the iteration starts. Then, $(\Sigma^{(k)})^{-1}\boldsymbol{h}^{(k)}$ simplifies to

$$(\Sigma^{(k)})^{-1}\boldsymbol{h}^{(k)}=\frac{R_{yy}^{-1}\boldsymbol{h}^{(k)}}{1-(\boldsymbol{h}^{(k)})^HR_{yy}^{-1}\boldsymbol{h}^{(k)}}. \quad (3.9b)$$

In the following, we discuss phase correction of the EM channel estimates.

A. Phase Correction

We describe a method for correcting the phases of the channel estimates in the EM iteration. Observe that the first product term in (3.3) is due to the unknown symbols, whereas the second term

$$\prod_{\tau=1}^{N_{\mathrm{T}}} f(\boldsymbol{y}_{\mathrm{T}}(\tau)|u_{\mathrm{T}}(\tau),\boldsymbol{h},\Sigma) \quad (3.10)$$

is due to the training symbols and is equal to the likelihood function for the case where *only* the training data are available. For i.i.d. constant-modulus symbols considered here [see (2.3)], the first term in (3.3) has M equal maxima (due to the phase ambiguity), which could cause the above EM iteration to converge to a local maximum of the likelihood function. We correct the phase of the EM channel estimates $\boldsymbol{h}^{(k)}$ to ensure that (3.10) is maximized. For example, for a quadrature phase-shift keying (QPSK) constellation, we find which of the four vectors — $\boldsymbol{h}^{(k)}, \boldsymbol{h}^{(k)}\exp(j\pi/2), \boldsymbol{h}^{(k)}\exp(-j\pi/2)$, and $\boldsymbol{h}^{(k)}\exp(j\pi)$ — maximizes the training-data likelihood function in (3.10) and update $\boldsymbol{h}^{(k)}$ accordingly. This test is computationally very efficient and may not need to be performed at every step of the EM iteration.

IV. Cramér–Rao Bound

We derive the CRB matrix for the unknown parameters under the measurement model in Section II. First, define the vector of the unknown channel and noise parameters $\boldsymbol{\zeta}=[\boldsymbol{\eta}^T,\boldsymbol{\psi}^T]^T$, where $\boldsymbol{\eta}=[\mathrm{Re}(\boldsymbol{h})^T,\mathrm{Im}(\boldsymbol{h})^T]^T$, and $\boldsymbol{\psi}=[\mathrm{Re}\{\mathrm{vech}(\Sigma)\}^T,\mathrm{Im}\{\underline{\mathrm{vech}}(\Sigma)\}^T]^T$. (The vech and $\underline{\mathrm{vech}}$ operators create a single column vector by stacking elements below the main diagonal columnwise; vech includes the main diagonal, whereas $\underline{\mathrm{vech}}$ omits it.) Define also the vector of the observed data

$$\boldsymbol{v}=\Big[\boldsymbol{y}(1)^T,\boldsymbol{y}(2)^T,\ldots,\boldsymbol{y}(N)^T\;\boldsymbol{y}_{\mathrm{T}}(1)^T,\boldsymbol{y}_{\mathrm{T}}(2)^T,\ldots,\boldsymbol{y}_{\mathrm{T}}(N_{\mathrm{T}})^T\Big]^T \quad (4.1a)$$

and the vector of the unobserved data

$$\boldsymbol{u} = [u(1), u(2), \ldots, u(N)]^T. \tag{4.1b}$$

Then, the CRB matrix for the unknown parameters $\boldsymbol{\zeta}$ is computed as (see [3, ch. 3.8.1]):

$$\mathrm{CRB}(\boldsymbol{\zeta}) = \left\{ \mathrm{E}_{\upsilon}[\boldsymbol{s}(\boldsymbol{\upsilon};\boldsymbol{\zeta})\boldsymbol{s}(\boldsymbol{\upsilon};\boldsymbol{\zeta})^T] \right\}^{-1} \tag{4.2}$$

where the expectation is performed with respect to the distribution of $\boldsymbol{\upsilon}$, and $\boldsymbol{s}(\boldsymbol{\upsilon};\boldsymbol{\zeta})$ is the observed-data score vector. The observed-data score vector can be computed as (see [3, eq. (3.42)])

$$\boldsymbol{s}(\boldsymbol{\upsilon};\boldsymbol{\zeta}) = \mathrm{E}_{u|\upsilon}[\boldsymbol{s}_c(\boldsymbol{\upsilon},\boldsymbol{u};\boldsymbol{\zeta})|\boldsymbol{\upsilon}] \tag{4.3}$$

where $\boldsymbol{s}_c(\boldsymbol{\upsilon},\boldsymbol{u};\boldsymbol{\zeta})$ is the complete-data score vector obtained by differentiating the complete-data log-likelihood function [i.e., the logarithm of (3.2)] with respect to $\boldsymbol{\zeta}$. Computing the expectations in (4.2) and (4.3) is discussed in Appendix B, where the expression for $\boldsymbol{s}_c(\boldsymbol{\upsilon},\boldsymbol{u};\boldsymbol{\zeta})$ is also given.

V. Detection

We now utilize the channel and noise estimates proposed in Section III to detect the unknown transmitted symbols $u(t)$. We apply the (estimated) maximum *a posteriori* (MAP) detector in (5.1), shown at the bottom of the page, where $\widehat{\boldsymbol{h}} = \boldsymbol{h}^{(\infty)}$ and $\widehat{\Sigma} = \Sigma^{(\infty)}$ are the ML estimates obtained from the EM iteration (3.4)–(3.5) upon convergence. To derive (5.1b), we have used the identity (3.9b) and the constant-modulus property of the transmitted symbols. Interestingly, the detector in (5.1b) is a function of the channel estimate $\widehat{\boldsymbol{h}}$ *only* through the $R_{yy}^{-1}\widehat{\boldsymbol{h}}$ term. Note that the above detection problem is equivalent to finding $m \in \{1, 2, \ldots, M\}$ that maximizes $\rho_m^{(\infty)}(t)$ in (3.8) [see also (3.4b)]. The detector (5.1) and EM algorithm (3.4)–(3.5) can be easily modified to account for unequal prior probabilities of the transmitted symbols.

VI. Simulation Results

We evaluate the performance of the proposed estimation and detection algorithms using numerical simulations. We consider an array of $n_{\mathrm{R}} = 5$ receiver antennas. Our performance metrics are the mean-square error (MSE) and symbol error rate (SER), averaged over 5000 random channel realizations generated using an i.i.d. Rayleigh fading model with unit-variance channel coefficients. The transmitted symbols were generated from an uncoded QPSK modulated constellation (i.e., $M = 4$) with normalized energy. We added a three-symbol training sequence ($N_{\mathrm{T}} = 3$), which was utilized to obtain the initial channel estimate $\boldsymbol{h}^{(0)}$, computed using least-squares estimation. The initial estimate of the noise covariance matrix was chosen as $\Sigma^{(0)} = R_{yy}$. The signal was corrupted by additive complex Gaussian noise with spatial covariance matrix Σ, whose (p,q)th element is

$$\Sigma_{p,q} = \sigma^2 \cdot 0.9^{|p-q|} \cdot \exp\left[j\left(\frac{\pi}{2}\right)(p-q) \right] \tag{6.1}$$

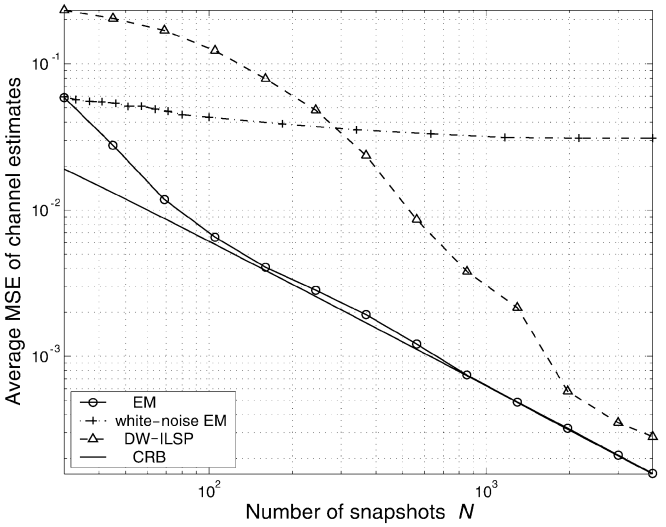

Fig. 1. Average mean-square errors and corresponding CRBs for the channel estimates obtained using the proposed EM algorithm, DW-ILSP method, and an EM algorithm for spatially white noise, as functions of N for $N_{\mathrm{T}} = 3$ and SNR $= -1$ dB.

which is the noise covariance model used in [22] (see also references therein). The bit signal-to-noise ratio (SNR) per receiver antenna was defined as

$$\mathrm{SNR} = 10\log_{10}\left[\frac{1}{\sigma^2 \cdot \log_2(M)}\right] = 10\log_{10}\left(\frac{1}{2\sigma^2}\right) \text{ (dB)}. \tag{6.2}$$

In the cases where the EM algorithm did not converge within 40 iterations, it was restarted using a randomly selected initial value for the channel coefficients.[2] [We implemented the same restart procedure in all algorithms whose performance is analyzed in this section.] We also applied the phase correction technique in Section III-A at every step of the EM iteration.

In the first set of simulations, the bit SNR was set to -1 dB. In Figs. 1 and 2, we show the average MSEs (and corresponding average CRBs) for the ML estimates of the channel coefficients[3] and selected elements of the spatial noise covariance matrix Σ (obtained using the proposed EM algorithm) as functions of the block length N. Fig. 1 also compares the MSE performance of the proposed EM algorithm with

- the decoupled weighted iterative least squares with projection (DW-ILSP) method in [23] and
- an EM algorithm that assumes spatially white noise.

For low SNR (-1 dB), few training symbols ($N_{\mathrm{T}} = 3$) and short block lengths, the proposed EM algorithm clearly outperforms the DW-ILSP method. In this scenario, the proposed method attains the CRB for $N = 100$ symbols, compared with more than 4000 symbols needed

[2]Note that fast convergence of the EM algorithm or utilizing the above restart method do not guarantee convergence to the global maximum of the observed-data likelihood function. Hence, our simulation results represent upper bounds on the performance achievable by the exact ML method.

[3]Here, averaging is performed over *both* the channel coefficients for different antennas (i.e., elements of $\widehat{\boldsymbol{h}}$) and random channel and training-data realizations.

$$\widehat{u}(t) = \arg\max_{u(t)\in\mathcal{U}} \frac{\exp\left\{-[\boldsymbol{y}(t) - \widehat{\boldsymbol{h}}u(t)]^H \widehat{\Sigma}^{-1}[\boldsymbol{y}(t) - \widehat{\boldsymbol{h}}u(t)]\right\}}{\sum_{n=1}^{M} \exp\left\{-[\boldsymbol{y}(t) - \widehat{\boldsymbol{h}}u_n]^H \widehat{\Sigma}^{-1}[\boldsymbol{y}(t) - \widehat{\boldsymbol{h}}u_n]\right\}}$$

$$= \arg\min_{u(t)\in\mathcal{U}} [\boldsymbol{y}(t) - \widehat{\boldsymbol{h}}u(t)]^H \widehat{\Sigma}^{-1}[\boldsymbol{y}(t) - \widehat{\boldsymbol{h}}u(t)] \tag{5.1a}$$

$$= \arg\max_{u(t)\in\mathcal{U}} \mathrm{Re}\left\{\boldsymbol{y}(t)^H R_{\boldsymbol{yy}}^{-1}\widehat{\boldsymbol{h}} \cdot u(t)\right\} \tag{5.1b}$$

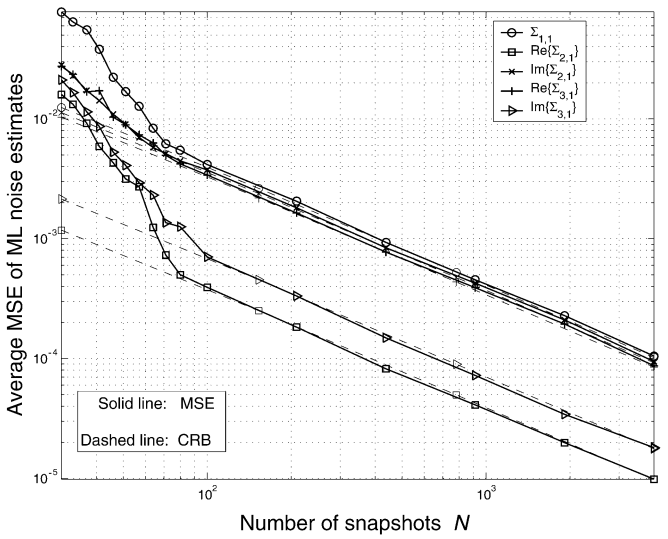

Fig. 2. Average mean-square errors and corresponding CRB for the ML estimates of $\Sigma_{1,1}$, $\mathrm{Re}\{\Sigma_{2,1}\}$, $\mathrm{Im}\{\Sigma_{2,1}\}$, $\mathrm{Re}\{\Sigma_{3,1}\}$, $\mathrm{Im}\{\Sigma_{3,1}\}$ obtained using the proposed EM algorithm, as functions of N for $N_{\mathrm{T}} = 3$ and SNR $= -1$ dB.

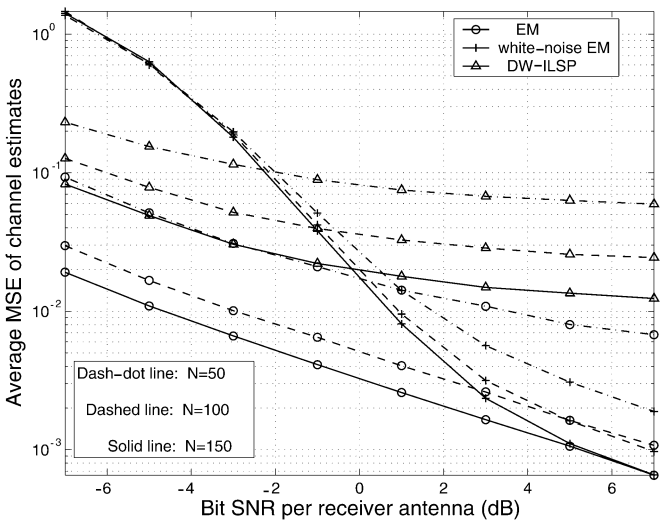

Fig. 3. Average MSEs for the channel estimates obtained using the proposed EM algorithm, DW-ILSP method, and EM algorithm for spatially white noise, as functions of the bit SNR per receiver antenna for block lengths $N = 50$, 100, and 150.

for the DW-ILSP method. [Note also that in fading channels, the block length N is limited by the coherence time of the channel.] The average numbers of iterations needed for the EM, white-noise EM, and DW-ILSP algorithms to converge were 9, 9, and 6, respectively. For $N = 100$, restart was needed in less than 0.1% of the total number of trials. A single EM iteration has higher computational complexity than a DW-ILSP iteration for the same N, and the complexity of both iterations increases linearly with N. However, the proposed EM algorithm typically needs a smaller N to attain the same MSE. To demonstrate the importance of incorporating the spatial color of the noise in channel estimation, we also show the performance of an EM algorithm that assumes spatially white noise in the scenario where the noise is *colored* [with covariance (6.1)]. The EM algorithm for spatially white noise follows from (3.4)–(3.5) by substituting $\Sigma^{(k)} = (\widehat{\sigma}^2)^{(k)} I_{n_{\mathrm{R}}}$ into Step 1 in (3.4) and applying the following Step 2: $(\widehat{\sigma}^2)^{(k+1)} = \mathrm{tr}(\Sigma^{(k+1)})/n_{\mathrm{R}}$, where $\Sigma^{(k+1)}$ was defined in (3.5), and $I_{n_{\mathrm{R}}}$ denotes the identity matrix of size n_{R}. For low SNR (-1 dB) and few training symbols ($N_{\mathrm{T}} = 3$), the white-noise EM algorithm breaks down.

In Fig. 2, we show the average MSEs for the ML estimates of $\Sigma_{1,1}$, $\mathrm{Re}\{\Sigma_{2,1}\}$, $\mathrm{Im}\{\Sigma_{2,1}\}$, $\mathrm{Re}\{\Sigma_{3,1}\}$, and $\mathrm{Im}\{\Sigma_{3,1}\}$ (obtained using the proposed EM algorithm) and the corresponding CRBs as functions of N.

In Fig. 3, the average MSEs for the channel estimates obtained by the proposed EM algorithm for spatially correlated noise, the DW-ILSP method, and the EM algorithm for spatially white noise are shown as functions of the bit SNR per receiver antenna for block lengths $N = 50$, 100, and 150. When the average MSE is 0.03 and $N = 100$, the EM algorithm has an advantage of about 9 dB over the DW-ILSP algorithm; this advantage further grows as N decreases. An intuitive explanation for this performance improvement is that the EM algorithm exploits additional information provided by the prior distribution of the unknown symbols in (2.3). Note also that the number of parameters in the random-symbol measurement model in Section II equals $n_{\mathrm{R}}^2 + 2n_{\mathrm{R}}$, and, therefore, is independent of N. This is in contrast with the DW-ILSP and other deterministic ML methods (e.g., [24]; see also [25]), where the number of parameters grows with N. For low SNRs, the white-noise EM algorithm performs poorly; see also Fig. 1. However, for high SNRs and small block lengths, it outperforms the EM algorithm for spatially correlated noise. Hence, in this scenario, the fact that the white-noise EM algorithm estimates a small number of parameters $(2n_{\mathrm{R}} + 1)$ becomes more important than accounting for

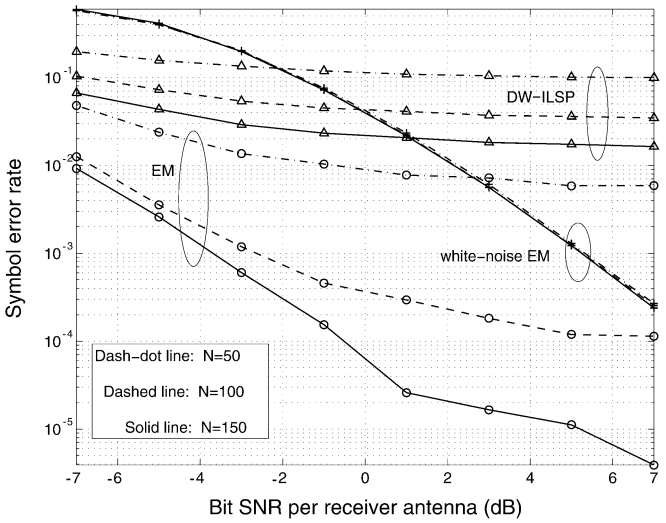

Fig. 4. Symbol error rates of the EM-based and DW-ILSP detectors, as functions of the bit SNR per receiver antenna for block lengths $N = 50$, 100, and 150.

spatial noise covariance (which, in addition, is poorly estimated due to the small block length).

In Fig. 4, we compare symbol error rates of the detector (5.1) that uses the ML estimates of $\boldsymbol{h}$ and Σ [obtained from the EM iteration (3.4) and (3.5)] with

- the DW-ILSP detector in [23] and
- a white-noise detector

$$\arg \max_{u(t)\in\mathcal{U}} \mathrm{Re}\left\{\boldsymbol{y}(t)^H \widehat{\boldsymbol{h}}_{\mathrm{white\ EM}} \cdot u(t)\right\} \tag{6.3}$$

where $\widehat{\boldsymbol{h}}_{\mathrm{white\ EM}}$ is computed using the EM algorithm for spatially white noise.

The symbol error rates are shown as functions of the bit SNR per receiver antenna for block lengths $N = 50$, 100, and 150. For the given range of SNRs and block lengths, the proposed detector significantly outperforms the DW-ILSP detector. As expected, the white-noise detector performs poorly for low SNRs due to poor channel estimates provided by the white-noise EM algorithm. Similarly, for high SNRs and small block lengths, it outperforms the detector in (5.1) due to the

fact that the white-noise EM algorithm outperforms the EM algorithm for spatially correlated noise in this scenario. The performance of the detector (5.1) improves significantly as the block length increases due to the improved channel estimation. In contrast, the performance of the white-noise detector is insensitive to the choice of the block length (for the block lengths considered in Fig. 4), which can be explained by the fact that the white-noise EM algorithm estimates a small number of parameters (and thus requires a relatively small data size).

VII. Concluding Remarks

We developed an expectation-maximization algorithm for semi-blind estimation of single-input multi-output fading channels in spatially correlated noise having unknown covariance. We also derived a method for phase correction of the EM channel estimates and computed the Cramér–Rao bounds for the unknown parameters. The proposed channel and noise estimators were incorporated into the receiver design. We presented numerical simulations that demonstrated the performance of the proposed methods and compared them with the existing techniques.

Further research will include extending the proposed methods to the multi-input multi-output (MIMO) scenario and reducing their computational complexity. For coded transmission, we will develop iterative schemes that combine EM channel estimation with decoding under the correlated noise scenario, generalizing the white-noise based methods in, e.g., [26] and [27].

Appendix A
EM Algorithm Derivation

We relax the constant-modulus assumption (2.2b) and first derive the EM algorithm for the general case where the symbols $u(t)$, $t = 1, 2, \ldots, N$, $u_{\mathrm{T}}(\tau)$, $\tau = 1, 2, \ldots, N_{\mathrm{T}}$ belong to an arbitrary constellation. This algorithm is then simplified to the constant-modulus scenario in Sections II and III.

By taking the logarithm of (3.2) and neglecting terms that do not depend on the parameters $\boldsymbol{h}$ and Σ, we obtain the complete-data log-likelihood function

$$\mathcal{L}(\boldsymbol{h},\Sigma) = -(N+N_{\mathrm{T}}) \cdot \left\{ \ln|\Sigma| + \mathrm{tr}\left[\Sigma^{-1}\cdot\left(R_{yy} - \boldsymbol{r}_{yu}\boldsymbol{h}^H - \boldsymbol{h}\boldsymbol{r}_{yu}^H + r_{uu}\boldsymbol{h}\boldsymbol{h}^H\right)\right]\right\} \tag{A.1}$$

where $|\cdot|$ denotes the determinant, and

$$R_{yy} = \frac{1}{N+N_{\mathrm{T}}}\left[\sum_{t=1}^{N}\boldsymbol{y}(t)\boldsymbol{y}(t)^H + \sum_{\tau=1}^{N_{\mathrm{T}}}\boldsymbol{y}_{\mathrm{T}}(\tau)\boldsymbol{y}_{\mathrm{T}}(\tau)^H\right] \tag{A.2a}$$

$$\boldsymbol{r}_{yu} = \frac{1}{N+N_{\mathrm{T}}}\left[\sum_{t=1}^{N}\boldsymbol{y}(t)u(t)^* + \sum_{\tau=1}^{N_{\mathrm{T}}}\boldsymbol{y}_{\mathrm{T}}(\tau)u_{\mathrm{T}}(\tau)^*\right] \tag{A.2b}$$

$$r_{uu} = \frac{1}{N+N_{\mathrm{T}}}\left[\sum_{t=1}^{N}|u(t)|^2 + \sum_{\tau=1}^{N_{\mathrm{T}}}|u_{\mathrm{T}}(\tau)|^2\right] \tag{A.2c}$$

are the *natural complete-data sufficient statistics* for estimating $\boldsymbol{h}$ and Σ; see, e.g., [16]. At the kth iteration, the E step computes the conditional expectation of the complete-data log-likelihood given the observed data $\boldsymbol{v}$ [see (4.1a)] at the current parameter estimates $\boldsymbol{h}^{(k)}$ and $\Sigma^{(k)}$:

$$Q(\boldsymbol{h},\Sigma;\boldsymbol{h}^{(k)},\Sigma^{(k)}) = -(N+N_{\mathrm{T}}) \cdot \left\{ \ln|\Sigma| + \mathrm{tr}\left[\Sigma^{-1}\cdot\left(R_{yy} - \boldsymbol{r}_{yu}^{(k)}\boldsymbol{h}^H - \boldsymbol{h}(\boldsymbol{r}_{yu}^{(k)})^H + r_{uu}^{(k)}\boldsymbol{h}\boldsymbol{h}^H\right)\right]\right\} \tag{A.3}$$

where

$$\boldsymbol{r}_{yu}^{(k)} = \mathrm{E}_{u|v}[\boldsymbol{r}_{yu}|\boldsymbol{v};\boldsymbol{h}^{(k)},\Sigma^{(k)}]$$

and

$$r_{uu}^{(k)} = \mathrm{E}_{u|v}[r_{uu}|\boldsymbol{v};\boldsymbol{h}^{(k)},\Sigma^{(k)}].$$

The above expression is obtained from (A.1) by replacing $\boldsymbol{r}_{yu}$ and r_{uu} with their conditional expectations $\boldsymbol{r}_{yu}^{(k)}$ and $r_{uu}^{(k)}$. The M step maximizes the above Q function with respect to $\boldsymbol{h}$ and Σ to produce

$$\boldsymbol{h}^{(k+1)},\Sigma^{(k+1)} = \arg\max_{\boldsymbol{h},\Sigma} Q(\boldsymbol{h},\Sigma;\boldsymbol{h}^{(k)},\Sigma^{(k)}). \tag{A.4}$$

The maximization of $\mathcal{L}(\boldsymbol{h},\Sigma)$ in (A.1) with respect to $\boldsymbol{h}$ and Σ has well-known solutions given by $\boldsymbol{r}_{yu}/r_{uu}$ and $R_{yy} - \boldsymbol{r}_{yu}\boldsymbol{r}_{yu}^H/r_{uu}$ (respectively), provided that $R_{yy} - \boldsymbol{r}_{yu}\boldsymbol{r}_{yu}^H/r_{uu}$ is a positive definite matrix; see, e.g., [18] and [19, Th. 10.1.1]. [These expressions follow from the multivariate analysis of variance (MANOVA) model in multivariate statistical analysis; see [18] and [19].] Hence, the M step is obtained by replacing $\boldsymbol{r}_{yu}$ and r_{uu} in $\boldsymbol{r}_{yu}/r_{uu}$ and $R_{yy} - \boldsymbol{r}_{yu}\boldsymbol{r}_{yu}^H/r_{uu}$ with their conditional expectations, and the EM iteration follows.

Step 1)

$$\boldsymbol{h}^{(k+1)} = \frac{1}{N+N_{\mathrm{T}}} \times \frac{\left\{\sum_{t=1}^{N}\left[\boldsymbol{y}(t)\sum_{m=1}^{M}u_m^*\cdot\rho_m^{(k)}(t)\right] + \sum_{\tau=1}^{N_{\mathrm{T}}}\boldsymbol{y}_{\mathrm{T}}(\tau)u_{\mathrm{T}}(\tau)^*\right\}}{r_{uu}^{(k)}} \tag{A.5a}$$

where

$$r_{uu}^{(k)} = \frac{1}{N+N_{\mathrm{T}}}\left\{\sum_{t=1}^{N}\sum_{m=1}^{M}\left[|u_m|^2\cdot\rho_m^{(k)}(t)\right] + \sum_{\tau=1}^{N_{\mathrm{T}}}|u_{\mathrm{T}}(\tau)|^2\right\}. \tag{A.5b}$$

Step 2)

$$\Sigma^{(k+1)} = R_{yy} - r_{uu}^{(k)}\cdot\boldsymbol{h}^{(k+1)}(\boldsymbol{h}^{(k+1)})^H \tag{A.6}$$

where $\rho_m^{(k)}(t)$ is computed using (3.4b). Note that (A.5) and (A.6) each incorporate both the E and M steps. Condition (3.7) is needed to ensure that $\Sigma^{(k+1)}$ is a positive definite matrix with probability one, which follows using arguments similar to those in [19, Th. 3.1.4]; see also [18, eq. (4)] and [19, Th. 10.1.1].

In the constant-modulus scenario (2.2b), we have that $r_{uu}^{(k)} \equiv 1$ for all k. Hence, setting $r_{uu}^{(k)} = 1$ in (A.5) and (A.6) yields the EM iteration (3.4) and (3.5).

Appendix B
Cramér–Rao Bound

We present the expression for the complete-data score vector $\boldsymbol{s}_c(\boldsymbol{v},\boldsymbol{u};\boldsymbol{\zeta})$ under the measurement model (2.1)–(2.3) and discuss evaluating the expectations in (4.2) and (4.3) that are needed to compute the CRB matrix. The complete-data score vector $\boldsymbol{s}_c(\boldsymbol{v},\boldsymbol{u};\boldsymbol{\zeta})$ for this measurement model is obtained by differentiating the complete-data log-likelihood function (A.1) with respect to $\boldsymbol{\zeta}$ (see [21, App. 15C]) and setting $r_{uu} = 1$:

$$\boldsymbol{s}_c(\boldsymbol{v},\boldsymbol{u};\boldsymbol{\zeta}) = \Big[\mathrm{Re}\left\{\boldsymbol{s}_{c,h}(\boldsymbol{v},\boldsymbol{u};\boldsymbol{\zeta})\right\}^T \; \mathrm{Im}\left\{\boldsymbol{s}_{c,h}(\boldsymbol{v},\boldsymbol{u};\boldsymbol{\zeta})\right\}^T, \boldsymbol{s}_{c,\psi}(\boldsymbol{v},\boldsymbol{u};\boldsymbol{\zeta})^T\Big]^T \tag{B.1}$$

where

$$\begin{aligned}\boldsymbol{s}_{c,h}(\boldsymbol{v},\boldsymbol{u};\boldsymbol{\zeta}) &= 2\cdot\Sigma^{-1}\cdot\left\{\sum_{t=1}^{N}[\boldsymbol{y}(t)u(t)^{*}-\boldsymbol{h}]\right.\\ &\qquad\left.+\sum_{\tau=1}^{N_{\mathrm{T}}}[\boldsymbol{y}_{\mathrm{T}}(\tau)u_{\mathrm{T}}(\tau)^{*}-\boldsymbol{h}]\right\}\\ &= 2\cdot(N+N_{\mathrm{T}})\cdot\Sigma^{-1}\cdot(\boldsymbol{r}_{yu}-\boldsymbol{h}) \qquad \text{(B.2a)}\end{aligned}$$

$$\begin{aligned}[\boldsymbol{s}_{c,\psi}(\boldsymbol{v},\boldsymbol{u};\boldsymbol{\zeta})]_i =& -(N+N_{\mathrm{T}})\cdot\mathrm{tr}\left(\Sigma^{-1}\frac{\partial\Sigma}{\partial\psi_i}\right)\\ &+(N+N_{\mathrm{T}})\cdot\boldsymbol{h}^{H}\Sigma^{-1}\frac{\partial\Sigma}{\partial\psi_i}\Sigma^{-1}\boldsymbol{h}\\ &+\sum_{t=1}^{N}\boldsymbol{y}(t)^{H}\Sigma^{-1}\frac{\partial\Sigma}{\partial\psi_i}\Sigma^{-1}\boldsymbol{y}(t)\\ &+\sum_{\tau=1}^{N_{\mathrm{T}}}\boldsymbol{y}_{\mathrm{T}}(\tau)^{H}\Sigma^{-1}\frac{\partial\Sigma}{\partial\psi_i}\Sigma^{-1}\boldsymbol{y}_{\mathrm{T}}(\tau)\\ &-\boldsymbol{h}^{H}\Sigma^{-1}\frac{\partial\Sigma}{\partial\psi_i}\Sigma^{-1}\cdot\sum_{t=1}^{N}[\boldsymbol{y}(t)u(t)^{*}]\\ &-\sum_{t=1}^{N}[\boldsymbol{y}(t)^{H}u(t)]\cdot\Sigma^{-1}\frac{\partial\Sigma}{\partial\psi_i}\Sigma^{-1}\boldsymbol{h}\\ &-\boldsymbol{h}^{H}\Sigma^{-1}\frac{\partial\Sigma}{\partial\psi_i}\Sigma^{-1}\cdot\sum_{\tau=1}^{N_{\mathrm{T}}}[\boldsymbol{y}_{\mathrm{T}}(\tau)u_{\mathrm{T}}(\tau)^{*}]\\ &-\sum_{\tau=1}^{N_{\mathrm{T}}}\left[\boldsymbol{y}_{\mathrm{T}}(\tau)^{H}u_{\mathrm{T}}(\tau)\right]\cdot\Sigma^{-1}\frac{\partial\Sigma}{\partial\psi_i}\Sigma^{-1}\boldsymbol{h}\\ =&(N+N_{\mathrm{T}})\\ &\cdot\left\{-\mathrm{tr}\left(\Sigma^{-1}\frac{\partial\Sigma}{\partial\psi_i}\right)\right.\\ &\quad+\mathrm{tr}\left(\Sigma^{-1}\boldsymbol{h}\boldsymbol{h}^{H}\Sigma^{-1}\frac{\partial\Sigma}{\partial\psi_i}\right)\\ &\quad+\mathrm{tr}\left(\Sigma^{-1}R_{yy}\Sigma^{-1}\frac{\partial\Sigma}{\partial\psi_i}\right)\\ &\quad-\mathrm{tr}\left[\left(\Sigma^{-1}\boldsymbol{r}_{yu}\boldsymbol{h}^{H}\Sigma^{-1}\right.\right.\\ &\quad\left.\left.+\Sigma^{-1}\boldsymbol{h}\boldsymbol{r}_{yu}^{H}\Sigma^{-1}\right)\cdot\frac{\partial\Sigma}{\partial\psi_i}\right]\Big\}. \qquad \text{(B.2b)}\end{aligned}$$

for $i=1,2,\ldots,n_{\mathrm{R}}^{2}$. To compute (B.2b), the following identities can be utilized:

$$\mathrm{tr}\left(A\cdot\frac{\partial\Sigma}{\partial\Sigma_{p,p}}\right)=A_{p,p},\quad p=1,2,\ldots,n_{\mathrm{R}} \qquad \text{(B.3a)}$$

and

$$\mathrm{tr}\left(A\cdot\frac{\partial\Sigma}{\partial\,\mathrm{Re}\{\Sigma\}_{p,q}}\right)=2\,\mathrm{Re}\{A_{p,q}\} \qquad \text{(B.3b)}$$

$$\mathrm{tr}\left(A\cdot\frac{\partial\Sigma}{\partial\,\mathrm{Im}\{\Sigma\}_{p,q}}\right)=2\,\mathrm{Im}\{A_{p,q}\} \qquad \text{(B.3c)}$$

for $1\le q<p\le n_{\mathrm{R}}$, where A is an arbitrary $n_{\mathrm{R}}\times n_{\mathrm{R}}$ Hermitian matrix. It follows from (B.2) that computing the observed-data score vector $\boldsymbol{s}(\boldsymbol{v};\boldsymbol{\zeta})$ in (4.3) reduces to replacing $\boldsymbol{r}_{yu}$ in (B.2) with its conditional expectation given $\boldsymbol{v}$:

$$\begin{aligned}\mathrm{E}_{u|v}[\boldsymbol{r}_{yu}|\boldsymbol{v}] =& \frac{1}{N+N_{\mathrm{T}}}\left\{\sum_{t=1}^{N}\left[\boldsymbol{y}(t)\sum_{m=1}^{M}u_m^{*}\cdot\rho_m(t)\right]\right.\\ &\left.+\sum_{\tau=1}^{N_{\mathrm{T}}}\boldsymbol{y}_{\mathrm{T}}(\tau)u_{\mathrm{T}}(\tau)^{*}\right\} \qquad \text{(B.4a)}\end{aligned}$$

where

$$\rho_m(t)=\frac{\exp\left\{-[\boldsymbol{y}(t)-\boldsymbol{h}u_m]^{H}\Sigma^{-1}[\boldsymbol{y}(t)-\boldsymbol{h}u_m]\right\}}{\sum_{n=1}^{M}\exp\left\{-[\boldsymbol{y}(t)-\boldsymbol{h}u_n]^{H}\Sigma^{-1}[\boldsymbol{y}(t)-\boldsymbol{h}u_n]\right\}}. \qquad \text{(B.4b)}$$

Finally, the CRB matrix is computed using (4.2), which requires multidimensional integration to evaluate the expectation with respect to the distribution of $\boldsymbol{v}$; this can be performed using Monte Carlo integration, i.e., by averaging $\boldsymbol{s}(\boldsymbol{v};\boldsymbol{\zeta})\boldsymbol{s}(\boldsymbol{v};\boldsymbol{\zeta})^{T}$ over many realizations of $\boldsymbol{v}$.

ACKNOWLEDGMENT

The authors are grateful to the anonymous reviewers for their helpful comments.

REFERENCES

[1] A. P. Dempster, N. M. Laird, and D. B. Rubin, "Maximum likelihood from incomplete data via the EM algorithm," *J. R. Stat. Soc.*, ser. B, vol. 39, pp. 1–38, July 1977.

[2] T. K. Moon, "The expectation-maximization algorithm," *IEEE Signal Processing Mag.*, vol. 13, pp. 47–60, Nov. 1996.

[3] G. J. McLachlan and T. Krishnan, *The EM Algorithm and Extensions*. New York: Wiley, 1997.

[4] M. J. Nissila, S. Pasupathy, and A. Mammela, "An EM approach to carrier phase recovery in AWGN channel," in *Proc. IEEE Int. Conf. Commun.*, Helsinki, Finland, June 2001, pp. 2199–2203.

[5] J. Qin, "Demodulation of binary PSK signals without explicit carrier synchronization," in *Proc. IEEE Int. Conf. Commun.*, Geneva, Switzerland, May 1993, pp. 498–501.

[6] C. N. Georghiades and D. L. Snyder, "The expectation-maximization algorithm for symbol unsynchronized sequence detection," *IEEE Trans. Commun.*, vol. 39, pp. 54–61, Jan. 1991.

[7] G. K. Kaleh and R. Vallet, "Joint parameter estimation and symbol detection for linear or nonlinear unknown channels," *IEEE Trans. Commun.*, vol. 42, pp. 2406–2413, July 1994.

[8] M. Shao and C. L. Nikias, "An ML/MMSE estimation approach to blind equalization," in *Proc. Int. Conf. Acoust., Speech, Signal Process.*, Adelaide, Australia, Apr. 1994, pp. IV/569–IV/572.

[9] H. A. Cirpan and M. K. Tsatsanis, "Stochastic maximum likelihood methods for semi-blind channel estimation," *IEEE Signal Processing Lett.*, vol. 5, pp. 21–24, Jan. 1998.

[10] Y. Li, C. N. Georghiades, and G. Huang, "Iterative maximum-likelihood sequence estimation for space-time coded systems," *IEEE Trans. Commun.*, vol. 49, pp. 948–951, June 2001.

[11] B. Lu, X. Wang, and Y. Li, "Iterative receivers for space-time block-coded OFDM systems in dispersive fading channels," *IEEE Trans. Wireless Commun.*, vol. 1, pp. 213–225, Apr. 2002.

[12] C. Cozzo and B. L. Hughes, "Joint channel estimation and data detection in space-time communications," *IEEE Trans. Commun.*, vol. 51, pp. 1266–1270, Aug. 2003.

[13] C. H. Aldana, E. de Carvalho, and J. Cioffi, "Channel estimation for mutilcarrier multiple input single output systems using the EM algorithm," *IEEE Trans. Signal Processing*, vol. 51, pp. 3280–3292, Dec. 2003.

[14] J. Míguez and L. Castedo, "Semiblind space-time decoding in wireless communications: A maximum likelihood approach," *Signal Process.*, vol. 82, pp. 1–18, Jan. 2002.

[15] H. A. Çirpan, E. Panayirci, and E. Çekli, "Maximum likelihood blind channel estimation for space-time coding systems," *EURASIP J. Appl. Signal Process.*, vol. 5, pp. 497–506, May 2002.

[16] P. J. Bickel and K. A. Doksum, *Mathematical Statistics: Basic Ideas and Selected Topics*, 2nd, Ed. Upper Saddle River, NJ: Prentice-Hall, 2000.

[17] A. Dogandžić, W. Mo, and Z. Wang, "Maximum likelihood semi-blind channel and noise estimation using the EM algorithm," in *Proc. 37th Annu. Conf. Inform. Sci. Syst.*, Baltimore, MD, Mar. 2003, pp. WA3.1–WA3.6.

[18] A. Dogandžić and A. Nehorai, "Generalized multivariate analysis of variance: A unified framework for signal processing in correlated noise," *IEEE Signal Processing Mag.*, vol. 20, pp. 39–54, Sept. 2003.

[19] R. J. Muirhead, *Aspects of Multivariate Statistical Theory*. New York: Wiley, 1982.

[20] D. A. Harville, *Matrix Algebra From a Statistician's Perspective*. New York: Springer-Verlag, 1997.

[21] S. M. Kay, *Fundamentals of Statistical Signal Processing: Estimation Theory*. Englewood Cliffs, NJ: Prentice-Hall, 1993, pt. I.
[22] M. Viberg, P. Stoica, and B. Ottersten, "Maximum likelihood array processing in spatially correlated noise fields using parameterized signals," *IEEE Trans. Signal Processing*, vol. 45, pp. 996–1004, Apr. 1997.
[23] A. Ranheim, "A decoupled approach to adaptive signal separation using an antenna array," *IEEE Trans. Veh. Technol.*, vol. 48, pp. 676–682, May 1999.
[24] N. Seshadri, "Joint data and channel estimation using blind trellis search techniques," *IEEE Trans. Commun.*, vol. 42, pp. 1000–1011, Feb.–Apr 1994.
[25] A. Dogandžić and A. Nehorai, "Finite-length MIMO adaptive equalization using canonical correlation analysis," *IEEE Trans. Signal Processing*, vol. 50, pp. 984–989, Apr. 2002.
[26] Z. Baranski, A. M. Haimovich, and J. Garcia-Frias, "EM-based iterative receiver for space-time coded modulation with noise variance estimation," in *Proc. Globecom Conf.*, Taipei, Taiwan, R.O.C., Nov. 2002, pp. 355–359.
[27] R. R. Lopes and J. R. Barry, "Exploiting error-control coding in blind channel estimation," in *Proc. Globecom Conf.*, San Antonio, TX, Nov. 2001, pp. 1317–1321.

Robust FIR Filter Design with Envelope Constraints and Channel Uncertainty

Ching-Min Lee and I-Kong Fong

***Abstract*—In this note, a finite impulse response (FIR) filter design problem is considered. The signals to be filtered are assumed to be corrupted by the channel noise. In addition, the channel characteristics are assumed to contain uncertainties. The linear matrix inequalities approach is adopted to provide two optimization procedures for designing H_∞ optimal filters and robust H_∞ filters subject to filter output envelope constraints. A numerical example is presented to illustrate the proposed filter design methods.**

***Index Terms*—Bounded stability, integral quadratic constraints, linear matrix inequality, robust FIR filter, time-domain envelope constraint.**

I. Introduction

In the field of signal processing, many filter design problems can be cast as constrained optimization problems. The constraints are usually defined by the specifications of the desired filters, and these specifications arise either from the standards set by certain regulatory bodies or from practical considerations. The time-domain envelope-constrained filter design is one example of these problems, which often involve requirements on the transient responses, such as the pulse-shape requirements in digital data transmission systems. In particular, these kinds of filters may be seen in applications like the pulse compression for many communication and radar systems, the TV waveform equalization with respect to the K-mask, and the data channel equalization or deconvolution, [1]–[3].

As to the optimization part, the H_∞ optimization theory has been widely used in robust control and signal processing problems [4]–[8].

Manuscript received Janary 4, 2003; revised July 21, 2003. This work was supported by the National Science Council of the Republic of China under Grant NSC 90-2213-E-002-084. The associate editor coordinating the review of this manuscript and approving it for publication was Dr. Yuan-Pei Lin.

The authors are with the Department of Electrical Engineering, National Taiwan University, Taipei, Taiwan 10617, R.O.C. (e-mail: d8921011@ee.ntu.edu.tw; ikfong@cc.ee.ntu.edu.tw).

Digital Object Identifier 10.1109/TSP.2004.827142

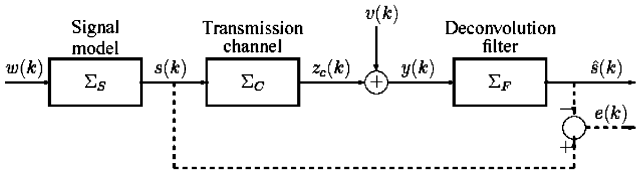

Fig. 1. Deconvolution filtering system.

Take the deconvolution filter design, for example. The objective of the problem may be set to the minimization of the H_∞ norm of the filtering error transfer function. In this approach, the system formulation allows the inclusion of the transmission channel and/or signal models. In addition, by utilizing methods developed in [7] and [9], the time-domain envelope constraints may be accommodated simultaneously. However, there are still other important factors to take care of, such as the system uncertainties. In the literature [10], [11], there are some discussions about input uncertainty of the filter, but consideration of input uncertainty bounds only [11] does not fully use information about system uncertainties that may be available. A more direct and complete approach for handling the transmission channel model uncertainties is desirable.

In this correspondence, the H_∞ optimal finite impulse response (FIR) filtering problem with envelope constraints and channel uncertainties is studied. The linear matrix inequality (LMI) framework is adopted, and the uncertainties in the channel are formulated as satisfying the integral quadratic constraints (IQCs) [12], [13]. The design method is also enhanced to ensure that the output of the filter is not too close to the constraining envelopes [8], [10], [14]. Compared with some existing method [14], which deals with the output envelope constraint problem by optimization procedures depending on the quasi-Newton method and golden section method, the LMI-based method handling a convex optimization problem is numerically more attractive. To illustrate the effectiveness of the proposed design method, a numerical example is presented.

II. Problem Formulation

Consider the deconvolution filtering system shown in Fig. 1. In the system, the source signal $s(k) \in \mathcal{R}$ is assumed to be generated by the signal model

$$\Sigma_S : \begin{cases} x_s(k+1) = A_s x_s(k) + B_s w(k) \\ s(k) = C_s x_s(k) + D_s w(k) \end{cases} \tag{1}$$

where $x_s(k) \in \mathcal{R}^{n_s}$ is the model state vector, $w(k) \in l_2[0,\infty)$ is the driving signal of the model, and A_s, B_s, C_s, and D_s are known constant matrices of appropriate dimensions. The source signal is transmitted through a channel with an uncertain characteristic modeled by

$$\Sigma_C : \begin{cases} x_c(k+1) = A_c x_c(k) + B_c s(k) + \sum_{i=1}^{p} H_{c1i}\xi_{ci}(k) \\ z_c(k) = C_c x_c(k) + D_c s(k) + \sum_{i=1}^{p} H_{c2i}\xi_{ci}(k) \end{cases} \tag{2}$$

where $x_c(k) \in \mathcal{R}^{n_c}$ is the channel state vector, $\xi_{ci}(k) \in \mathcal{R}^{n_i}$, $i = 1, 2, \ldots, p$ is the ith uncertain vector satisfying the IQC [12]

$$\sum_{k=0}^{\mu} \|\xi_{ci}(k)\|^2 \le \sum_{k=0}^{\mu} \|E_{1i}x_c(k) + E_{2i}s(k) + E_{3i}\xi_c(k)\|^2 \tag{3}$$

as $\mu \to \infty$, $\xi_c^T(k) = [\xi_{c1}^T(k) \ \cdots \ \xi_{cp}^T(k)]$, and A_c, B_c, C_c, D_c, H_{c1i}, H_{c2i}, E_{1i}, E_{2i}, and E_{3i} are known constant matrices with appropriate dimensions. For subsequent usage, we define $H_{c1} = [H_{c11} \ \cdots \ H_{c1p}]$, $H_{c2} = [H_{c21} \ \cdots \ H_{c2p}]$, $E_1^T = [E_{11}^T \ \cdots \ E_{1p}^T]$, $E_2^T = [E_{21}^T \ \cdots \ E_{2p}^T]$, and $E_3^T = [E_{31}^T \ \cdots \ E_{3p}^T]$.